Modeling current and voltage peaks generation in complementary resistive switching devices

S. Blonkowski, M. Labalette, S. Jeannot, S. Ecoffey, A. Souifi, D. Drouin

Version of Record: https://www.sciencedirect.com/science/article/pii/S0038110121001659
Manuscript_a1b3be8e5f4e4f14c9bb6405613b0e8b

Modeling Current and Voltage peaks generation in Complementary Resistive Switching devices

S. Blonkowski[1], M. Labalette[2,3,4], S. Jeannot[3], S. Ecoffey[2], A. Souifi[2,4], D. Drouin[2]
[1]*Université Grenoble Alpes CEA Leti Grenoble, France*
[2]*Laboratoire Nanotechnologies Nanosystemes (LN2) - CNRS UMI-3463, Université de Sherbrooke, Québec, Canada*
[3]*STMicroelectronics Crolles, France*
[4]*Institut des Nanotechnologies de Lyon (INL) – Villeurbanne, France*
E-mail address of corresponding author: serge.blonkowski@cea.fr

***Abstract*—We propose a physical model of complementary resistive switching (CRS) based on the disruption and reformation process of a metallic filament inside each Oxyde Resistive Random Access Memory (OxRRAM) composing the CRS. The driving forces involved in this process are electromigration forces, electron phonon coupling and joule heating. The model accounts well for the experimental CRS current voltage characteristics. The stability of the CRS states and the CRS operation in pulse regime, including the current and voltage peaks generation are discussed.**

Keywords—Complementary resistive switching (CRS), resistive random access memory (RRAM), non-volatile memory (NVM)

Complementary Resistive Switching (CRS) devices are interesting candidates for the reductions of sneak path currents in passive crossbar OxRRAM (Oxide Resistive Random Access Memory) matrices [1, 2] and present crossbar logic operation capabilities [3]. They consist in the anti-serial connection of two OxRRAM junctions. The CRS acts as both selector and local current limiter. CRS models for Electrochemical Metallization Cells (ECM) association [6,7] as Valence Change Memories(VCM) [8] already exist. OxRRAM based CRS have also been modelled assuming that the filamentary switching mechanism is attributed to the action of the electric field on oxygen vacancies and ions [9,10]. Some recent experiments on TiN/HfO_x/Ti structures based on TEM observations [11] and conductive AFM tips EDX measurements [12] show that a Ti filament appears during the forming step. Since the electrical field in metals is zero the above-mentioned mechanisms are more than questionable in our structure. An approach, which takes into account those considerations reproduces satisfactorily OxRRAM operation in many conditions [13]. The model developed here addresses the coupling between two OxRRAM in an anti-serial configuration, each described by the model derived in [13]. In particular, one found that this coupling induces current and voltage peak generation. This feature is useful to provide neuron spike output generation, which is an important feature in neuromorphic silicon neuron circuits [14].

II. Model and Comparison with Experience

A. Experimental structure and model description

SEM top-view of CRS devices made using the BEOL compatible *nanodamascene* process [4, 5] including an anti-serial configuration TiN/HfO_x/Ti MIM structures is shown in figure 1(a). In figure 1(b) one can see a schematic representation of the two OxRRAM from figure 1(a) with their metallic filaments labelled P and Q in blue. The filaments are larger (cross section area S_0) near the Ti central electrode and present nanometric constrictions with maximum area Sc that can be filled or emptied with metal atoms in the zone labelled (1) from the zone labelled (2) in Figure 1 (b). The constrictions are located at distances Zcp and Zcq from the central Ti electrode.

The CRS time evolution is described by a system of two balance equations governing the time evolution of the two state variables P and Q that represent the occupation probability by Ti atoms of each OxRRAM constriction. In the following indexes P and Q refers to OxXRAM P and Q.

$$\begin{cases} \frac{dQ}{dt} = k_{2Q}(1-Q) - k_{1Q}Q \\ \frac{dP}{dt} = k_{2P}(1-P) - k_{1P}P \end{cases} \quad (1)$$

The transfer rates k_{1P} k_{1Q} ,k_{2P} , k_{2Q} can be expressed as:

$$\begin{cases} k_{1P} = \tau_0^{-1} e^{-\frac{W_1 + d.F_1}{k_b T p(Vp,P,Q)}} \\ k_{1Q} = \tau_0^{-1} e^{-\frac{W_1 - d.F_1}{k_b T q(Vq,P,Q)}} \end{cases} \quad (2a)$$

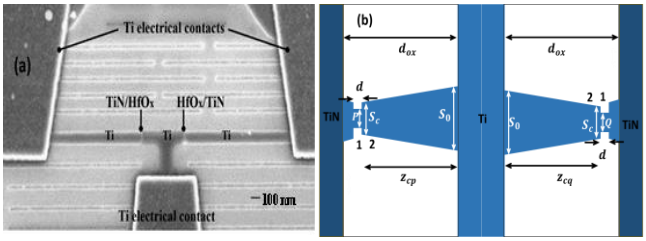

Fig. 1 a) SEM top-view of a CRS device composed by two fully oxide buried Ti/HfO_x/TiN OxRRAM junctions after the CMP step of the *nanodamasecene* process. b) CRS Model consisting in two anti-serial OxRRAM according to the SEM top-view of figure 1a). Parameters are explained in the text and in table 1.

$$\begin{cases} k_{2P} = \tau_0^{-1} e^{-\frac{W_2 + d.F_2}{k_b T p(Vp,P,Q)}} \\ k_{2Q} = \tau_0^{-1} e^{-\frac{W_2 - d.F_2}{k_b T q(Vq,P,Q)}} \end{cases} \quad (2b)$$

In equation 2, τ_0 is the atomic vibration time (10^{-12} s), k_b is the Boltzmann constant, W_1 and W_2 the atomic potential well energy in the positions 1 and 2 respectively, d is the distance between the positions 1 and 2 (§ Figure 1(b)). F_2 and F_1 are the electromigration forces defined by equation 3.

$$F_{1,2} = 2mv_F \frac{\sigma}{q} J_{1,2} \eta_{1,2} \quad (3)$$

In equation 3, m and q are the electron mass and charge respectively, v_F the fermi velocity, σ an atomic cross section and J the electronic current density. The temperature due to Joule heating is [13]:

$$\begin{cases} Tjp(T,Vp) = T - \frac{I(Vp)^2}{2\kappa\sigma_c S_c}\left(2z_{cp}^2 - \frac{z_{cp}}{Tox}\left(z_{cp}^2 + dox^2\right)\right) - \frac{I(Vp)^2}{2\kappa\sigma_c S_0}\left(z_{cp}^2\left(\frac{z_{cp}}{dox} - 1\right)\right) \\ Tjq(T,Vq) = T - \frac{I(Vq)^2}{2\kappa\sigma_c S_c}\left(2z_{cq}^2 - \frac{z_{cp}}{dox}\left(z_{cq}^2 + dox^2\right)\right) - \frac{I(Vq)^2}{2\kappa\sigma_c S_0}\left(z_{cq}^2\left(\frac{z_{cq}}{dox} - 1\right)\right) \end{cases} \quad (4)$$

κ, σ_c the thermal and electrical conductivities of the metallic filament and T the external temperature (here 300K). $I(V_p)$ and $I(V_q)$ stand for the current as function of individual OxRRAM voltage V_p and V_q. However, when the contention is open (i.e. when P or Q = 0), considering Joule heating in the constriction is not relevant. In that case, the local electronic temperature in the constriction depends on the voltage with the following expression (§ [13] and references therein):

$$\begin{cases} Tep(T,Vp) = \frac{T}{1+\alpha} + \frac{\frac{qVp}{2k_B}\coth\left(\frac{qVp}{2k_BT}\right)}{1+\alpha^{-1}} \\ Teq(T,Vq) = \frac{T}{1+\alpha} + \frac{\frac{qVq}{2k_B}\coth\left(\frac{qVq}{2k_BT}\right)}{1+\alpha^{-1}} \end{cases} \quad (5)$$

In equation 5, α stands for the ratio of characteristic phonon and electron relaxation times.

The overall temperature is then the electronic contribution at the place where the constriction is empty and the Joule contribution in the filled place of the constriction:

$$\begin{cases} Tp(Vp,P,Q) = T_{Jp}(Vp,T)P + T_{ep}(Vp,T)(1-P) \\ Tq(Vq,P,Q) = T_{Jq}(Vq,T)Q + T_{eq}(Vq,T)(1-Q) \end{cases} \quad (6)$$

The conductance in the metallic filaments is described by the Sharvin conductance [13, 15]:

$$\begin{cases} Gp(P) = \frac{2q^2}{h}\frac{k_F^2 S_c P}{4\pi}\left(1 + \gamma\frac{3dox}{4\lambda}\right)^{-1} \\ Gq(Q) = \frac{2q^2}{h}\frac{k_F^2 S_c Q}{4\pi}\left(1 + \gamma\frac{3dox}{4\lambda}\right)^{-1} \end{cases} \quad (7)$$

In equation 7, h is the Plank constant k_F the Fermi wave vector, λ the electron mean free path and γ a geometric factor whose value is about 1. When P=1, $G(P)$=G_{on}. When the constriction is empty (i.e when P or Q=0) the current is assumed to be due to tunneling and the current is given by:

$$\begin{cases} Ip = G(P)Vp + (1-P)I_{tp}(Vp) \\ Iq = G(Q)Vq + (1-Q)I_{tq}(Vq) \end{cases} \quad (8)$$

The coupling of the dynamic system is due to the Kirchhoff voltage and current laws:

$$\begin{cases} V = Vp + Vq + Vs \\ Ip = Iq = \frac{Vs}{Rs} \end{cases} \quad (9)$$

In equation 9, V is the applied voltage, R_s and V_s are respectively, the serial resistance and the corresponding voltage drop. The self-consistent numerical resolution of equations 1 to 9 allows obtaining P and Q and then current voltage characteristics.

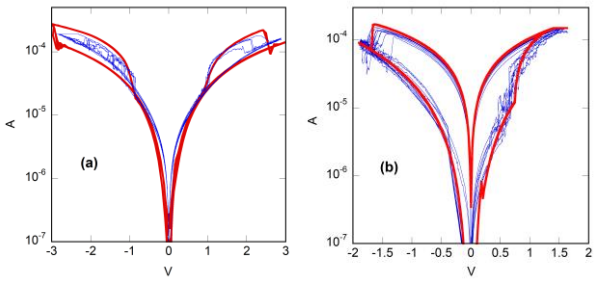

Fig. 2 a). Current versus applied voltage CRS resistive switching characteristics in voltage ramp condition. Experimental: Blue crosses. Model fitting with parameters of table 1: red line. (b) individual OxRRAM element Current versus voltage resistive switching characteristics in blue. Experimental, blue crosses. Model fitting with parameters of table 1: red crosses.

TABLE I

Symbol	Quantities	Values
Ef	Fermi Energy (Ti)	8.8 eV
ρ(Ti)	Density	4500 Kg.m^{-3}
K(Ti)	Filament Thermal conductivity	21 W/(K.m)
σ_c(Ti)	Filament conductivity	2.5 10^6 (Ω.m)$^{-1}$
γ	Geometric factor in conductance	1
α	Electron phonon coupling factor	0.1
λ	Electron mean free path	12.5 nm
d	Constriction thickness d	3 Å
Φ_b	Barrier Height	0.2 eV
V_1	Energy well of position 1	3 eV
V_2	Energy well of position 2	2.4eV
σ	Electromigration force cross section	2.9 10^{-16} cm²
z_{cp}, z_{cq}	Constrictions locations	9.3 Å - 9.4Å

B. Comparison with experimental characteristics

The physical quantities and the fitted parameters of the model fitting results of figures 2a and 2b are listed in Table 1. The filament physical quantities (Fermi wave vector κ_F, electrical conductivity σ_c, the thermal conductivity κ are those of Titanium consistently with our assumptions and are not fitting parameters. In order to calibrate the model one has to fix the Sc value. The On state conductance has been proved experimentally and theoretically to be proportional to the compliance current: Ic=GonVc [13] for an individual OxRRAM. Thus according to equation 7 with P=1 we have:

$$Gon = \frac{2q^2}{h}\frac{k_F^2 S_c}{4\pi}\left(1 + \gamma\frac{3Tox}{4l}\right)^{-1} = Ic/Vc \quad (10)$$

Where Vc = 0.35 V [13].. The value of Sc= 0.6 nm² was obtained from Gon= 5.43 10^{-4} S, which is consistent with the assumption of a small filament constriction with respect

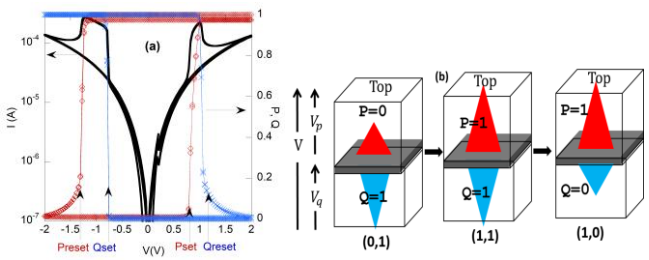

Fig. 3 a) Calculated current-applied voltage CRS resistive switching characteristics in voltage ramp condition and R_s =700 Ω (black with crosses) right ordinate. *P* (red line with diamonds) and *Q* (blue line with crosses) corresponding calculated values on left coordinate. (b) Schematic description of the CRS filaments corresponding to P and Q states.

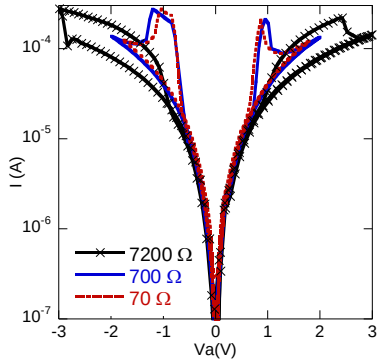

Fig. 4 Serial resistance (Rs) effect on current-applied voltage CRS resistive switching characteristics in voltage ramp condition. Rs=7200 Ω black line with crosses, R_s = 700 Ω blue line, R_s=70 Ω red dashed line

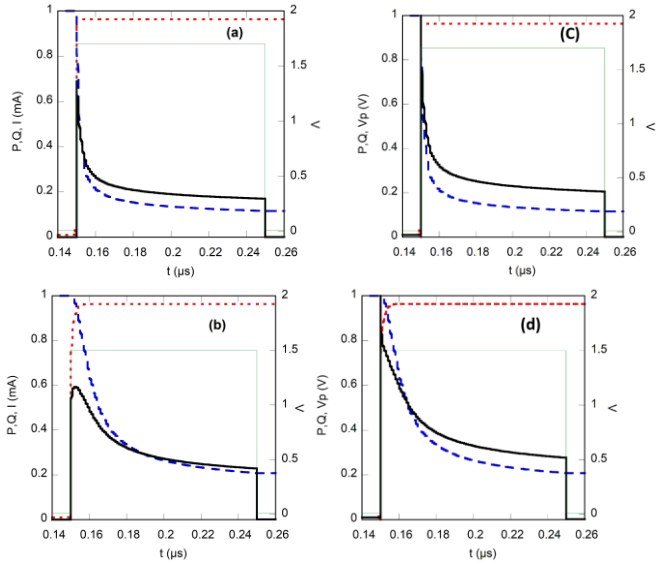

Fig.5 : Illustration of current and voltage spike generation by CRS: Calculated *P* (red dots), *Q* (blue dashed line) and current in mA (black thick line) on left ordinate vs time. For several Applied pulse voltage values 1.7V (a), 1.5 V (b) thin green lines on right ordinate. Calculated *P* (red dots), *Q* (blue dashed line) and Vp in Volts (black thick line) on left ordinate vs time. For several Applied pulse voltage values 1.7V (c), 1.5 V (d) thin green lines on right ordinate.

to the dimensions of our devices.

III. DISCUSSION

On Figure 3 (a) we reported the CRS current-voltage ramp switching characteristic. The ON state for the CRS (P,Q)=(1,1) correspond to voltage between the P_{RESET} and Q_{SET} negative voltages and P_{SET} and Q_{RESET} positive voltages. Outside of this domain the CRS is in (1,0) or (0,1) states. It appears that the situation $P = Q = 0$ is not observed. Let's assume that P = 1 and Q= 0 and Rs=0, thus $G_p > G_q$ and $V_p < V_q$ (since $V_pG_p=V_qG_q$). Now, for an individual OxRRAM (§figure 2b) the absolute value of the set voltage is always lower than the one of the RESET. *Q* will then set before *P* RESET and the CRS will be in the (1,1) state. The same argument holds for P = 1 and Q = 0. Thus states (1,0) or (0,1) can only switch to (1,1). Once in the (1,1) state the system can only switch to (1,0) or (0,1), because one OxRRAM has to RESET first. Thus the (0,0) state cannot be stable as already observed [2].

The apparent tight memory window observed in figures 2

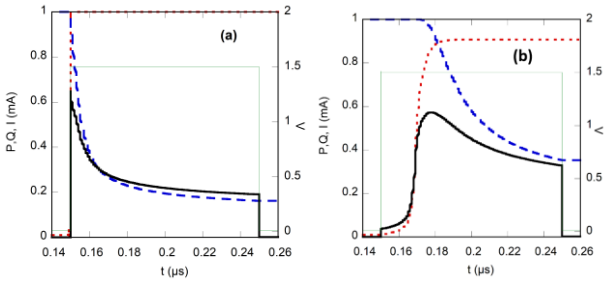

Fig.6: Illustration of electromigration force intensity on current spike generation by CRS. Calculated *P* (red dots), *Q* (blue dashed line) and current in mA (black thick line) on left ordinate vs time for several electromigration conditions at 1.5 V: 210% of the nominal force (a), 65% of the nominal force (b)

is due to the high serial resistance Rs=7200 Ω inherent to the TiN via access (§ figure 1 (a)). We illustrate the effect of serial resistance in figure 4 where the characteristic of figure 2 (a) is also calculated lowering the serial resistance by factors ~10 to 100. For the two lowest resistances values (700 and 70 Ω), one retrieves CRS switching characteristics comparable to published characteristics [10]. In the following for sake of clarity, we will consider the predictions of the model for resistances lower or equal to 700 Ω.

On Figure 5, we have simulated the response of the CRS to 1.7 V and 1.5V pulses during 100 ns. We set the Gon= 8.5710^{-4}S, Sc= 0.96 nm². Before the positive pulse, the state is (0,1). At t = 150 ns the application of the positive voltage pulse induces the (0,1)→(1,1)→(1,0) transition, which is schematized on figure 3 b. As one can see on figures 5 a) and d), that the application of 1.7 V pulse results in a current and voltage peak respectively (for the OxRRAM P). In the (1,1) state, Vp=Vq=V/2 (0.85V) reported on figure 5 (d) and I=Gon.V/2=730µA is the current peak value (§figure 5 a). During the transition (1,1)→(1,0) the conduction of the Q OxRRAM which resets limits the current because the Q constriction becomes the smallest as Q decreases. The reset transient of the current follows the one of the conductance

(~Gon.Q). The voltage peak is due to the divider bridge between P and Q. Neglecting the serial resistance and the tunneling current, Vp=Q.V/(P+Q). During the (1,1)→(1,0) transition, Vp decreases from V/2 because Q decreases from Q=1 while P=1.

If one lowers the voltage pulse, (1.5V fig 5 b, d) the current transient become smoother. The voltage pulse reduction smooth the time variation of P and Q mainly because of the temperature and electromigration forces reduction. On figure 6 we have reported the effect of the electromigration force variation. On both OxRRAMs the electromigration force was multiplied by the same factor while maintaining a 1.5V bias. Enhancing the electromigration force (with a 210% factor in this case) enhances in turn the sharpness of the current peak while reducing the force (65% of the force) reduces the sharpness and delays (~15ns) the transition time. As it is illustrated on figure 3 (b) a positive bias on the top electrode results in an electromigration force directed toward the top electrode. The force tends to fill the constriction Q during the transition (1,1)→(1,0). The force on Q is about 0.7 nN at 1.5 V (1 nN at 1.9V), which is the correct order of magnitude to modify the size of metallic nanoscale contact [15]. The force in the Q constriction is 10 time larger than in the P OxRRAM because during the transition Vq becomes larger than Vp (since Vp decreases §figures 5). Lowering this force results in reducing the probability to fill the constriction and the reset of Q needs more time. Conversely enhancing the force accelerate the reset of Q leading to a sharper pulse.

If one removes the electromigration force from the model, the transient behavior as the current and voltage peaks observed in figures 5 and 6 vanish. This is because the transitions are only due to the temperature changes, which have a brutal impact on the transfer coefficient. Because of the Arrhenius law, the temperature is in the denominator in the exponential in equations 2 leading to a sharp variation of transfer coefficient with voltage.

IV. CONCLUSION

The model reproduces successfully single device and CRS switching experimental characteristics in voltage sweep conditions. The model predicts that in the CRS, both OxRRAM cannot be simultaneously in high resistance state and that the transition between the On state and the Off state of the CRS is transient. The duration of this transient is mainly due to the action of the electromigration force. The pulse voltage allows driving the current spike shape and width.

The current and voltage peak generation predicted by the model can be useful for neuromorphic applications.

References

[1] G.W. Burr, R.H. Shenoy, K. Virwani, P. Narayan, A. Padilla, B. Kurdi, Access devices for 3D crosspoint memory, Review article, J. Vac. Sci. Technol. 040802-1(2014) [2] E. Linn, R. Rosezin, C. Kügeler, R. Waser, Complementary Resistive Switches for Passive Nanocrossbar Memories, Nature Material, 9,403 (2010) https://doi.org/10.1038/nmat2748

[2] E. Linn, R. Rosezin, C. Kügeler, R. [14] .Brandbyge, J Schiøtz, M.R. Sørrensen,P. Stoltze K.W.Jacobsen,J.K. Nørskov , L Olesen,E.Laegsgaard, I Stensgaard and F Besenbacher,1995 Quantized conductance in atom sized wires between two metals,Phys. Rev.B,**52**,8499,CrossrefGoogle Scholar

[3] R. Rosezin, E. Linn, C. Kügeler, R. Bruchhaus, R. Waser, Crossbar Logic Using Bipolar and Complementary Resistive Switches, IEEE, Electron. Dev. Lett. 32,6,710 (2011) 10.1109/LED.2011.2127439

[4] M. Labalette, S. Jeannot, S. Blonkowski, Y. Beilliard, S. Ecoffey, A. Souifi, D. Drouin, Fabrication of Planar Back End of Line Compatible HfOx Complementary Resistive Switches, IEEE Trans. Nanotech. 16, NO. 5, September 2017 10.1109/TNANO.2017.2698205

[5] M. Labalette, Intégration 3D de dispositifs mémoires résistives complémentaires dans le back-end-of-line du CMOS. Thèse de l'Université de Sherbrooke et INSA Lyon. (2018).

[6] E. Linn, S. Menzel, R. Rosezin, U. Böttger, R. Bruchahaus, R. waser, Modeling Complementary Resistive Switches by Nonlinear Memristive Systems, IEEE International Conference on Nanotechnology, Portland Oregon USA (2011) p 1474 **DOI:** 10.1109/NANO.2011.6144318

[7] Linn, E., Menzel, S., Ferch, S., & Waser, R. (2013). Compact modeling of CRS devices based on ECM cells for memory, logic and neuromorphic applications. *Nanotechnology*, *24*(38), 384008. https://doi.org/10.1088/0957-4484/24/38/384008

[8] A. Siemon, S. Menzel, A. Marchewka, Y. Nishi, R. Waser, E. Linn Simulation of TaOx-based Complementary Resistive switches by a physics-based Memristive model International Symposium on Circuits and Systems ICSAS Melbourne Vic Australia , p1420 (2014) DOI 10.1109/ISCAS.2014.6865411

[9] F. Nardi, S. Balatti,, S. Larentis, D.C. Gilmer, D. Ielmini, Complementary Switching in Oxide-based bipolar resistive-switching random memory IEEE Trans. Electron. Dev. 60,1,70 (2013) DOI**:** 10.1109/TED.2012.2226728

[10] Ambrogio, S., Balatti, S. Gilmer, D. C, Ielmini, D., (2014). Analytical Modeling of Oxide-Based Bipolar Resistive Memories and Complementary Resistive Switches. IEEE Transaction on Electron. Dev. ,61, 7, (2014) **DOI:** 10.1109/TED.2014.2325531

[11]T. Dewolf, V. Delaye, N. Bernier, D. Cooper, N. Chevalier, H. Grampeix, C. Charpin, E. Jalaguier, M. Kogelschatz, S. Schamm-Chardon, G. Audoit, Nano-characterization of switching mechanism in HfO_2-based oxide resistive memories by TEM-EELS-EDS, European Microscopy Congress 2016: Proceedings pp598-599 https://doi.org/10.1002/9783527808465.EMC2016.5934

[12] A.K. Singh, S. blonkowski, M. Kogelschatz, "Resistive switching study in HfO_2 based resistive memories by conductive atomic force microscopy in vacuum, J. Appl. Phys. 124,014501 (2018) https://doi.org/10.1063/1.5025143

[13] S. Blonkowski, T. Cabout, Bipolar resistive switching from liquid helium to room temperature, J. Phys. D, 48,34, 345101 (2015) https://doi.org/10.1088/0022-3727/48/34/345101

[14] Indiveri, G., Linares-Barranco, B., Hamilton, T. J., Schaik, A.

van, Etienne-Cummings, R., Delbruck, T., … Boahen, K. (2011). Neuromorphic silicon neuron circuits. *Frontiers In Neuroscience*, *5*(73). https://doi.org/10.3389/fnins.2011.00073

[15] .Brandbyge, J Schiøtz, M.R. Sørrensen,P. Stoltze K.W.Jacobsen,J.K. Nørskov , L Olesen,E.Laegsgaard, I Stensgaard and F Besenbacher,1995 Quantized conductance in atom sized wires between two metals,Phys. Rev.B,**52**,8499,CrossrefGoogle Scholar